Surface Properties of Ti_2AlV (100) and (110) Surfaces Using First-Principle Calculations

David. M. Tshwane* *and Rosinah* Modiba

Future Production: Manufacturing, Advanced Materials Engineering, CSIR, PO Box 395, Pretoria, 0001, South Africa

Abstract. Ti_2AlV alloys are commonly employed as structural materials in electronics, metallurgy, and other industries because of their outstanding properties. Knowledge about their surface properties is lacking and limited at the atomic level. In this work, structural, electronic, and stabilities of Ti_2AlV surfaces were investigated using the density functional theory approach. This study also looked at the surface energies and work functions of various surfaces. According to our findings, it was found that the (110) surface is thermodynamically stable with lower surface energy than the (100) surface. It was discovered that the surface energy increases with regard to the thickness of the surface slab. Furthermore, the work function of the (110) surface was found to be increasing than that of the (100) surface. Moreover, the work function was found to increase with increasing number of layers in both surfaces. The partial and total density of states of Ti_2AlV (100) and (110) were also studied. It was also found that the Fermi level lies at the minimum curve in the TDOS graphs for the Ti_2AlV (110) surface while lies at the maximum in (100) surface.

Introduction

Ti-Al-V alloys have become the most used titanium alloys, with high strength, low density, great fracture toughness, and outstanding corrosion resistance [1]. These light and robust alloys reduce weight in heavily stressed structures and are ideal for a wide range of components, such as gas turbines, automobiles, energy, chemical and biomedical industries [2, 3]. However, these materials have inherent constraints such as surface roughness, porosity, and a high affinity for oxygen [4]. Which this surface instability and roughness limits the materials application. Material surface properties that are highly repeatable and stable are required in several disciplines of scientific study and industrial production operations [5].

Rafi *et al.* [6] examined the surface roughness of Ti-Al-V components made, it was reported that the surface roughness is caused by differences in scan speeds, powder size, and layer heights. Li *et al.* [7], mentioned that the surface roughness is formed by three main courses: the higher layer number caused by the staircase, exterior surface adhesion of partly melted powder, the presence of open pores and partially melted areas. In addition, it was reported that the surface roughness decreases as the powder feed rate is reduced and as the

* Corresponding author : DTshwane@csir.co.za

scan speed is increased. Low surface roughness is typically necessary to provide greater functionality, for most of its material applications, in ceramic and metal machining [8].

Theoretical work in the past has been focused on predicting the stable surfaces of MAX (where M represents transition metal, A is a group element and X is carbon and nitrogen), the majority of these studies have concentrated mainly on (001) surfaces [9, 10]. Because of their critical involvement in the process of surface oxidation, understanding the low index surface structures of Ti-Al-V and characteristics of metallic or intermetallic alloys is critical [10]. Among other studies, based on calculating the surface energies of M_2AlC surfaces (M= Ti, V and Cr). The corresponding surface energy of Al and M(C) terminated (0001) surface was found to be more stable while for Cr_2AlV only the Al terminated was reported to be stable [11].

Zhou *et al.* [12] used the first-principle approach to investigate the low-index surface properties of Al_3Ti. The calculated surface energies of Al_3Ti surfaces in this study revealed that the most stable surface was a nonstoichiometric (110) surface with an Al termination. Furthermore, the chemical potential of Al increased the surface energy of nonstoichiometric surfaces of TiAl-terminated surfaces, whereas it decreased the surface energy of Al-terminated surfaces [12]. The surface stabilities of (100), (110), and (111) surfaces of the ɣ-TiAl alloy were previously studied and investigated using the density functional theory (DFT) method. It was also reported elsewhere that the stoichiometric (100) surface is the most stable, and additionally that the Al terminated (110) surface becomes more stable as the Al chemical potential increases [13]. Gertzen *et al.* [14] employed the DFT method to investigate MAX phase surfaces of (Ti_2AlC, Ti_3AlC_2 and Ti_3SiC) for electrocatalyst support material in hydrogen fuel cells. It was reported that the cleavage energy value for Ti_2AlC is lower (1.924 to 5.254 eV/unit cell) than Ti_3AlC_2 (1.9-6.48 eV/unit cell) and Ti_3SiC_2 (2.8-6.47 eV/unit cell) surfaces.

Moreover, the first-principles approach was previously used to evaluate the surface stability of Ti_2AlNb surfaces [15]. The estimated surface energies showed that the most stable surface of Ti_2AlNb is the stoichiometric (010) surface. In addition, the reported surface energies range between 1.96-2.72 J/m^2. Also, among the considered surfaces, the surface energies of Ti terminated, Ti and Nb stoichiometric were relatively higher [15]. More importantly, it was stated that the atomic termination has a significant impact on the surface stability of Ti_2AlNb [16] and it was also consisted with previous research on TiAl surfaces. Consequently, the Al and Ti stoichiometric surfaces (100) and (111) are more stable than the Al or Ti terminated surfaces [17]. Several studies have reported and carried out to investigate various surface stability on the polycrystalline surfaces, such as Ti_2AlNb [16], Ti_2AlC [18], ɣ-TiAl (001) and (100) surfaces [19]. However, there is lack of literature on surface stability of Ti_2AlV surfaces that has been reported. In this work, surface properties of Ti_2AlV (100) and (110) surfaces were investigated using DFT. The surface energy, work function, and density of states at various surface terminations and layers were calculated to identify the most preferred surface.

Methodology

In this work, First principle calculations were performed using Cambridge Sequential Total Energy Package (CASTEP) code [20], in a plane-wave pseudopotential approach [21] as implemented on BOIVIA Materials Studio Software, (MS 2020 version). For the exchange-correlation functional, a generalized gradient approximation with Perdew-Burke-Erzernhof (PBE) parameterization was used [22]. In all surface calculations a cutoff energy of 500 eV for the plane-wave basis set and a 4x4x1 Monkhorst-Pack [23] K-point were utilized. The Broyden-Fetcher-Goldforb-Shanno minimizations scheme algorithm was used during optimization of geometry. The convergence tolerance and absolute maximum force were set

to 1x10^{-5} eV/atom and 0.03 eV/Å, respectively. A periodic slab with a finite slab and 30 Å vacuum layers was used to replicate surface calculations. The Ti_2AlV (100) and (110) surfaces with 3-5 atomic layers and different termination (TiAl, TiV, TiAlV) were considered in this study. The symmetric side view of an atomic structure for (a) (100) TiV termination, (b) (100) TiAl termination and (c) Ti_2AlV (110) surfaces with 5 atomic layers is presented in Figure 1, in this order. Figure 1(a-b) shows that the Ti_2AlV (100) surface has two terminations (the TiAl and TiV atomic layers shown in the first two figures), whereas the Ti_2AlV (110) surface has only one termination (TiAlV layer).

The thermodynamic surface stability is decided by determining the surface energy, which is regarded to be an important factor and is defined as:

$$\gamma = \frac{1}{2A}\left(E_{surf} - NE_{bulk}\right) \quad (1)$$

where E_{surf} and E_{bulk} correspond to the total energies of the Ti_2AlV slab and bulk whilst A and N represent the area and number of atoms on the surface; respectively. The slab is surrounded by two symmetric surfaces, which accounts for 1/2 factor in this equation.

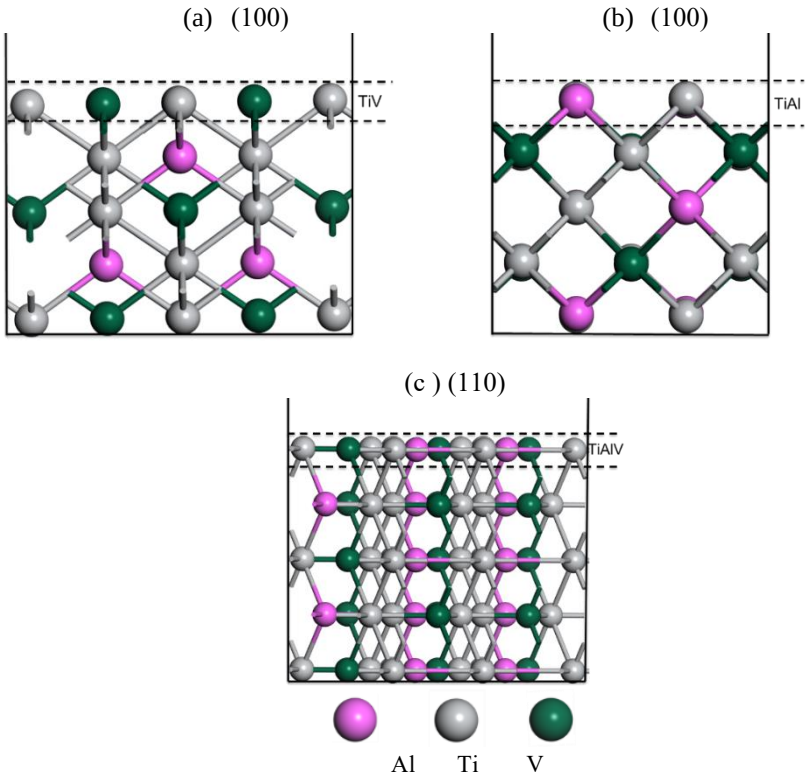

Fig. 1. Side view of atomistic structures of Ti_2AlV: (a-b) (100) surfaces and (c) (110) surface.

The work function (Φ) is an important aspect to consider when analyzing metallic surfaces, normally known as electrostatic potential. The minimal energy necessary to remove an electron from a metallic surface to a distance in a vacuum is specified as the work function and is described using the expression:

$$\Phi = E_{vac} - E_{F,} \quad (2)$$

where E_{vac} and E_F represent the electrostatic potential energy of the vacuum and Fermi energy level, respectively.

Results and Discussion

Surface Energy

Surface properties are particularly important because of their wide range of applications, including catalysis. Moreover, theoretical analysis of metallic surfaces requires extensive knowledge of electronic structures [24]. The surface energies of low-index surfaces were calculated using equation 1. The surface energy of Ti_2AlV (100) and (110) surfaces based on different atomic layers and terminations were computed and the results are presented in Table 1. Calculated surface energies of the Ti_2AlV (110) surface were found varying from 0.172 to 0.208 J/m^2 which is lower than the surface energy values (0.228 to 1.253 J/m^2) of (100) surface for TiAl terminations. This is consistent with the surface energies of 1.21 J/m^2 reported by Liu *et al.* [25] on ɣ-TiAl surfaces. As shown in Table 1 (100) surface possess two terminations slab (TiAl and TiV). We did notice, however, that the TiV termination on the (100) surface has negative surface energy values for both the 5 and 3 layers. This implies that the (100) surface stability of Ti_2AlV structure is strongly dependent on the atomic termination. The TiV termination surface form V rich slab which contribute to the high total energy than the bulk and resulted in the negative surface energies. On the other hand, it is significant to remember that the surface energy changes to a negative value when chemical effects are considered [26]. According to other research by, Magomedov [27] extremely severe uniform compression or tension is the cause of the negative value of surface energy. Furthermore, it was discovered that the surface energy strength decreases with regard to the thickness of the surface slab for (110) surface. It was found that 5 atomic layers on (110) surfaces have lower surface energy than 3 and 4 atomic layers. However, for (100) surface energy increases differ in number of layers wherein the 4 layers of TiAl/TiV termination slab shows lower surface energy as compared to 5 and 3 layers. The Ti and Al stoichiometric was discovered to be more stable than Ti and V termination indicating that the atomic termination has a very influence over the surface stability. However, there is a scarcity of Ti_2AlV surface energies in the literature.

Table 1. Calculated surface energies (ɣ) (J/m^2) of Ti_2AlV (100) and (110) surfaces.

surfaces	terminations	layers	ɣ(J/m^2)
100	TiAl	5	1.253
		4	0.228
		3	0.874
	TiV	5	-0.833
		4	0.228
		3	-1.469
110	TiAlV	5	0.172
		4	0.179
		3	0.208

Work Function

Work function is the most fundamental crystal solid surface parameter for comprehending a wide range of structural, physical, and chemical surface conditions [28]. The computed work function of Ti_2AlV (100) and (110) surfaces were calculated using equation 2. Figure 2(a-b) demonstrates the schematic plot for the work function of Ti_2AlV (100) and (110) surfaces, respectively. The difference between the surface's vacuum potential and the Fermi energy level is defined as the estimated work function or electrostatic potential of a solid surface [29]. The electrostatic energy value is mainly determined by the charge rearrangement of electrons and ions near the surface. The work function of the metal surface generally depends on the crystalline orientation of the surface, indicating that the work function of different surfaces can differ slightly.

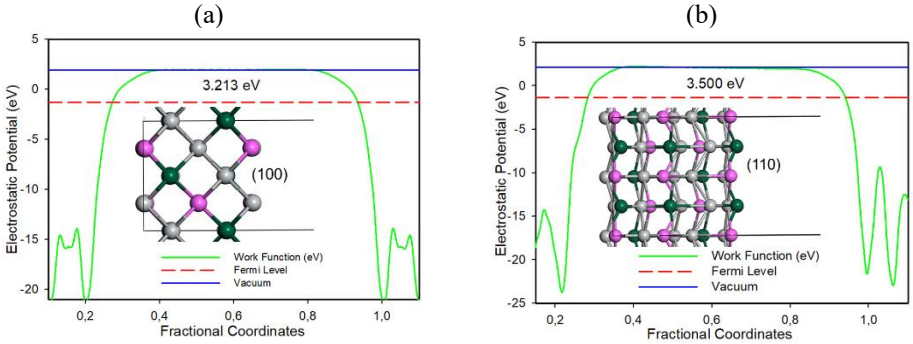

Fig. 2. Present the schematic plots of the work function (Φ) along with the slab models: (a) Ti_2AlV (100) and (b) Ti_2AlV (110) surface.

The computed work function values for the (100) surface vary from 3.213 to 3.524 eV (TiAl and TiV termination), whereas the work function for the (110) surface is 3.375 to 3.500 eV for 3 to 5 layers. The Φ value difference between both surfaces has a magnitude of ~0.16 eV and ~0.024 eV which is influenced by surface atomic termination and relaxation. It was noted that the work function of (110) has a much larger numerical value than that of the (100) surface as shown Figure 2. The atomic charge rearrangement and electron redistribution cause a difference in work function. The redistribution of d electrons on metal surfaces affects work function, and these changes in the work function differ from one surface to another [30]. Importantly, the surface with a lower work function value suggests a higher and easier electron extraction. This implies that the Ti_2AlV (100) surface will lose electrons easier than the (110) surface.

Density of States

The density of states (DOS) was computed to investigate the atomic bonding between Ti, Al and V atoms, and electronic interaction between the atomic orbitals. The partial density of states (PDOS) plots of Ti_2AlV (100) and (110) surfaces are shown in Figure 3. The zero on the energy x-axis represents the Fermi energy (E_F). Electronic PDOS peaks for Al atoms in both surfaces is shown in Figure 3, (top panels) which is mainly consist of s- and p- orbital states. Also, the PDOS peaks for Ti and V atoms in (100) and (110) surfaces are seen in Figure 3, (middle and bottom panels, respectively) with predominantly d- orbital states contribute more, while s- and p- orbitals contribute less at the E_F. This clearly indicates a strong metallic character of Ti_2AlV surfaces. Moreover, the hybridization is observed at around -3 eV and -5 eV which emanates from the s-p orbitals of Al atom and -d orbital from

both Ti and V atoms as seen on Figure 3a and 3b. This shows atomic bonding between Ti-Al and V-Al bonds.

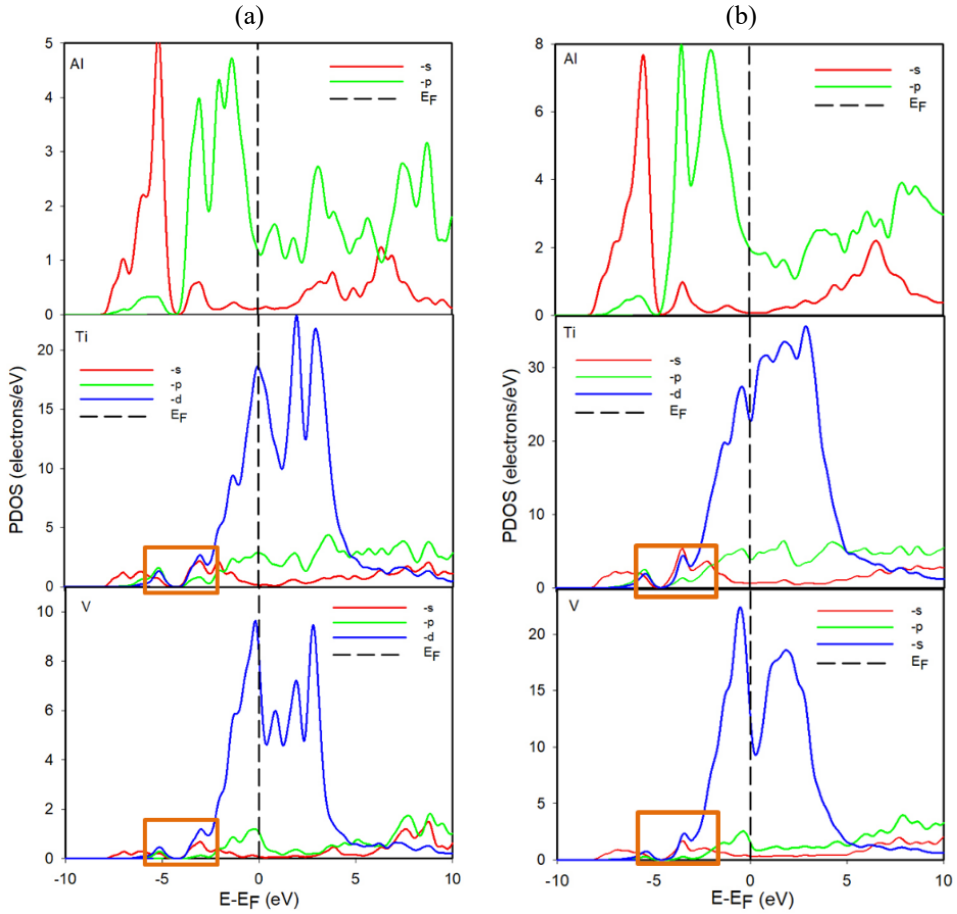

Fig. 3. Present the partial density of states (PDOS) for Ti_2AlV (a) (100) and (b) (110) surfaces.

In addition, Figure 4 presents the embedded total density of states (TDOS) for both (100) and (110) surfaces. The TDOS plots show closely the pattern of the -d orbital contributing more towards the Fermi level as mentioned on Figure 3. It was also observed that the Fermi level lies in the minimum curve in the TDOS graphs for the Ti_2AlV (110) surface. However, a (100) surface Fermi level with TiAl termination lies at the maximum curve, whereas TiV termination is in the middle of the TDOS curve. Surface local DOS changes are primarily related to charge redistribution near the surface and the appearance of surface states which concentrated near the Fermi level [19]. The difference in TDOS plots with regard to E_F implies that the (110) surface is more stable than (100) surface and confirms the surface energy stability observed in Table 1.

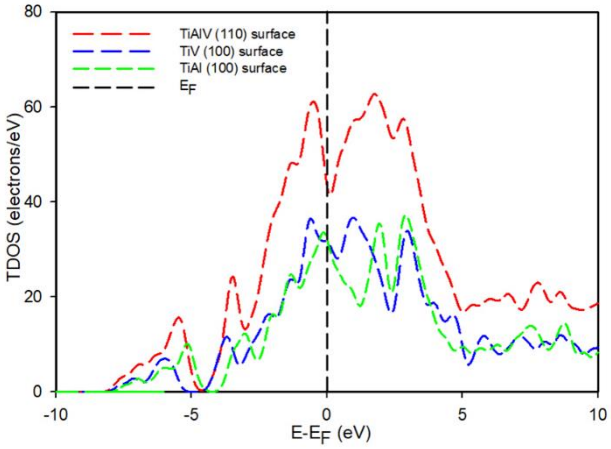

Fig. 4 : Total density of states (TDOS) for Ti_2AlV (100) and (110) surfaces.

Conclusion

The structural stability of Ti_2AlV (100) and (110) surfaces has been effectively explored using first-principle calculations. Evaluation of surface energy revealed that (110) surface is the most stable surface than (100) surface, implying that the (110) is thermodynamically more than the Ti_2AlV (100) surface. Results showed that the Ti_2AlV surface stability strength depends on the number of layers or thickness of the slab and atomic slab termination, with a 5 layers surface of (110) being the most stable. Moreover, the analysis reveals that the TiV termination on the (100) surface has negative surface energy while TiAl termination has positive surface energy. The work function analysis revealed that the value of the work function varies from one surface to the next and increases with increasing surface slab. Furthermore, it was also discovered that the Fermi level is in the minimum curve on the DOS graphs for the Ti_2AlV (110) surface. However, for (100) surface Fermi level with TiAl termination is at the maximum curve, whereas TiV termination is in the middle of the TDOS curve.

Acknowledgements

The authors acknowledge the Department of Science and Innovation (DSI) and Council for Scientific and Industrial Research for financial support. Center for High-Performance Computing for computing resources.

References

[1] C. Cui, B. Hu, L. Zhao, S. Liu, Mater. Des. **32**, 1684 (2011)

[2] R.R. Boyer, Mater. Sci. Eng. A, **213**, 103 (1996)

[3] P. Singh, H. Pungotra, N.S. Kalsi, Mater. Today Proc. **4**, 8971 (2017)

[4] S.S. Al-Bermani, M.L. Blackmore, W. Zhang, I. Todd, Metall. Mater. Trans. A **41**, 3422 (2010)

[5] T. Bodner, A. Behrendt, E. Prax, F. Wiesbrock, Monatsh, Chem. **143** 717 (2012)

[6] H.K. Rafi, N.V. Karthik, H. Gong, T.L. Starr, B.E. Stucker, J. Mater. Eng. Perform. **22**, 3872 (2013)

[7] P. Li, D.H. Warner, A. Fatemi N. Phan, Int. J. Fatigue **85**, 130 (2016)

[8] X. Song, X. Wang, S. Wang, S. Liu, S. Ge, Mater. **14**, 5014 (2021)

[9] Z. Sun, R. Ahuja, Appl. Phys. Lett. **88**, 161913 (2006)

[10] D. Music, Z. Sun, R. Ahuja, J.M. Schneider, Surf. Sci. **601**, 896 (2007)

[11] J. Wang, J. Wang, Y. Zhou. J. Phys.: Condens. Matter. **20**, 225006 (2008)

[12] Y. Zhou, H. Xiong, Y. Yinb, S. Zhong, RSC Adv. **9**, 1752 (2019)

[13] L. Wang, J.X. Shang, F.H. Wang, Y. Zhang, A. Chroneos, J. Phys.: Condens. Matter. **23**, 265009 (2011)

[14] J. Gertzen, P. Levecque, T. Rampai, T. van Heerden, Mater. **14**, 77 (2021)

[15] Y. Li, J. Dai, Y. Song, R. Yang, Comput. Mater. Sci. **139**, 412 (2017)

[16] Y. Li, J. Dai, Y.Song, J. Alloys Compd. **818**, 152926 (2020)

[17] Y. Song, J.H. Dai, R. Yang, Surf. Sci. **606**, 852 (2012)

[18] Q. Kang, G. Wang, Q. Liu, X. Sui, Y. Liu, Y. Chen, S. Luo. Z. Li, Corros. Sci. **191**, 109756 (2021)

[19] S.E. Kulkova, A.V. Bakulin, Q.M. Hu and R. Yang, Comput. Mater. Sci. **97**, 55 (2015)

[20] M.D. Segall, P.J.D. Lindan, M.J. Probert, C.J. Pickard, P.J. Hasnip, S.J. Clark, M.C. Payne, J. Phys.: Condens. Matter. **14**, 2717 (2002)

[21] G. Kresse, J. Joubert, Phys. Rev. B **59**, 1758 (1999)

[22] J.P. Perdew, K. Burke, M. Ernzerhof, Phys. Rev. Lett. **77**, 3865 (1996)

[23] H.J. Monkhorst, J.D. Pack, Phys. Rev. B **13**, 5188 (1976)

[24] A. Patra, J.E. Bates, J. Sun, J.P. Perdew, Proc. Natl. Acad. Sci. **114**, E9188 (2017)

[25] X. Liu, H. Dong, X. Lv, N. Hu, L. Wen, Z. Yang, Mol. Simul. **45**, 50 (2019)

[26] F. Lai, J. Phys.: Conf. Ser. **1759**, 012014 (2021)

[27] M. Magomedov, J. Surf. Investigation: X-ray, Synchrotron and Neutron Techniques **7**, 1114 (2013)

[28] C. Fall. PhD Thesis, 1-144 (1999)

[29] L. Markus. PhD Thesis, 1-117 (2003)

[30] C.J. Fall, N. Binggeli, A. Baldereschi, Phys. Rev. B **61,** 8489 (2000)